ELSEVIER

Buoyancy and thermocapillary driven convection flow of an electrically conducting fluid in an enclosure with heat generation

M. Anwar Hossain [a,*], M.Z. Hafiz [b], D.A.S. Rees [c]

[a] *Department of Mathematics, University of Dhaka, Dhaka 1000, Bangladesh*
[b] *Institute of Information Technology, University of Dhaka, Dhaka 1000, Bangladesh*
[c] *Department of Mechanical Engineering, University of Bath, Bath BA2 7AY, United Kingdom*

Abstract

The effect of surface tension on unsteady laminar natural convection flow of an electrically conducting fluid in a rectangular enclosure under an externally imposed magnetic field with internal heat generation has been investigated. The top horizontal surface of the rectangular cavity is assumed to be free and the bottom one insulated, whereas the left vertical wall is cold and the right one is uniformly hot. The equations are non-dimensionalized and solved numerically by an upwind finite difference method together with a successive over-relaxation (SOR) technique. The effects of heat generation together with the combined effects of the magnetic field and the surface tension are presented graphically in terms of isotherm and streamline plots. The effects of varying the physical parameters on the rate of heat transfer from the heated surface of the enclosure are also depicted. The fluid here has Prandtl number $Pr = 0.054$ which is representative of liquid metal and semiconductor melts.

1. Introduction

When a free surface is present in free convection flow of a liquid, variations in the surface tension at the free surface due to temperature gradients, can induce motion within the fluid. Such flow is known either as thermocapillary flow or Marangoni convection. Convective flows driven by both buoyancy and surface tension play an important role in the growth of crystals and in materials processing, especially in small-scale and low gravity hydrodynamics [1–3]. Combined buoyancy and thermocapillary convection flow or Marangoni convection flow in a differentially heated cavity has been investigated numerically by Bergman and Ramadhyani [4] who showed that surface tension alters significantly the resulting flow pattern. Srinivasan and

Basu [5] computed numerically thermocapillary flow in a rectangular cavity during laser melting. The gas–liquid interface was assumed to be flat with a sinusoidal variation of temperature. Thereafter Basu and Srinivasan [6] simulated numerically a two-dimensional steady state laser-melting problem in a cavity; while Chen and Huang [7] conducted a similar study with a moving heat flux along the free surface. Carpenter and Homsy [8] studied the problem of combined buoyancy thermocapillary convection flow in a square cavity with a free surface, which is heated differentially in the horizontal direction. The influence of thermocapillary forces on natural convection flow in a shallow cavity has also been investigated numerically by Hadid and Roux [9].

An externally imposed magnetic field is also a widely used tool for control of melt flow in the bulk crystal growth of semiconductors. One of the main purposes of electromagnetic control is to stabilize the flow and suppress oscillatory instabilities, which degrades the resulting crystal.

---

* Corresponding author.
E-mail address: anwar@udhaka.net (M.A. Hossain).

Nomenclature

$\mathbf{B}$	uniform magnetic field, $= B_x\mathbf{e}_x + B_y\mathbf{e}_y$
B_x, B_y	space independent components of $\mathbf{B}$ of constant magnitude
B_0	magnitude of $\mathbf{B}$
C_p	specific heat at constant pressure .. $\mathrm{J\cdot kg^{-1}\cdot K^{-1}}$
$\mathbf{e}_x, \mathbf{e}_y$	unit vectors in Cartesian coordinate system
$\mathbf{F}$	electromagnetic force
g	gravitational acceleration . . . . $\mathrm{m\cdot s^{-2}}$
Gr	Grashof number
H	enclosure height . . . . m
Ha	Hartmann number
$\mathbf{J}$	the electric current
K	effective thermal conductivity of the media . . . . $\mathrm{W\cdot m^{-1}\cdot K^{-1}}$
Ma	Marangoni number
Nu	Nusselt number
p	fluid pressure . . . . Pa
Pr	Prandtl number
t	time . . . . s
T	temperature . . . . °C
u	velocity in x-direction . . . . $\mathrm{m\cdot s^{-1}}$

v	velocity in y-direction . . . . $\mathrm{m\cdot s^{-1}}$
x, y	Cartesian coordinates . . . . m
X, Y	dimensionless coordinates
$\mathbf{V}$	field velocity ($u\mathbf{e}_x + v\mathbf{e}_y$)

Greek symbols

β	coefficient of thermal expansion of fluid .. $\mathrm{K^{-1}}$
θ	dimensionless temperature
λ	dimensionless heat absorption/generation parameter
ϕ	the orientation of the magnetic field with horizontal axis (such that $\tan\phi = B_y/B_x$)
φ	is the electric potential
μ	effective dynamic viscosity . . . . $\mathrm{Pa\cdot s^{-1}}$
ν	effective kinematic viscosity (μ/ρ)
ρ	fluid density at reference temperature (T_0)
σ	surface tension
γ	temperature coefficient
τ	dimensionless time
ψ	streamfunction . . . . $\mathrm{m^2\cdot s^{-1}}$
Ω	dimensionless vorticity

Numerous studies have already been devoted to the numerical modeling of electromagnetic stabilization of the convective flows in several different configurations [10–14]. In a recent article Gelfgat and Yoseph [15] studied the effect of an externally imposed magnetic field on the linear stability of steady convection flow in a horizontally elongated rectangular cavity for fluid having $Pr = 0.015$, which is associated with the horizontal Bridgman crystal growth process.

On the other hand, Rudraiah et al. [16] investigated the effect of surface tension on buoyancy driven flow of a electrically conducting fluid in a square cavity in the presence of a vertical transverse magnetic field to see how this force damps hydrodynamic movements; since, this is required to enhance crystal purity, increase compositional uniformity and reduce defect density. It should further be stated that natural convection heat transfer induced by internal heat generation has recently received considerable attention because of numerous applications in geophysics and energy-related engineering problems. Such applications include heat removal from nuclear fuel debris, underground disposal of radioactive waste materials, storage of food-stuff, and exothermic chemical reactions in packed-bed reactor (see, for instance, Kakac et al. [17]).

Acharya and Goldstein [18] studied numerically two-dimensional natural convection of air in an externally heated vertical or inclined square box containing uniformly distributed internal energy sources. Recently, Churbanov et al. [19] studied numerically unsteady natural convection of a heat generating fluid in a vertical rectangular enclo-

sure with isothermal or adiabatic rigid walls. Other related works dealing with temperature-dependent heat generation effects can be found in the works of Vajravelu and Nayfeh [20]. Recently, Chamkha and Naser [21] investigated the problem of unsteady, laminar, hydromagnetic, double-diffusive natural convection flow inside a rectangular enclosure in the presence of heat generation or absorption.

In the present investigation we have considered the problem on combined buoyancy and thermo-capillary convection flow of electrically conducting fluid filled in an enclosure under an externally imposed time-independent uniform magnetic field including the additional effect of internal heat generation. Numerical simulations of the governing equations have been carried out by employing an upwind finite difference method together with a successive over-relaxation (SOR) technique. For example, we have chosen a fluid that has a small Prandtl number (i.e., $Pr = 0.054$, which is appropriate for liquid metal and semi-conductor melts) and a Marangoni number ($Ma = 100$ and 1000) which depends on the thermocapillary force). Solutions of the problem in terms of streamlines, isotherms as well as heat transfer from the heated surface have been obtained for values of the Grashof number, Gr, equal to 2×10^4, 2×10^5 and 2×10^6, the Hartmann number, Ha, which depends on the transverse magnetic field, ranges from 0.0 to 40 and the heat generation parameter, λ, ranges from 0.0 to 40. A detailed development of the present investigation is given in the subsequent sections.

2. Mathematical formulation

Here we consider the unsteady two-dimensional natural convection flow of a fluid with kinematic viscosity μ, density ρ, thermal diffusivity α and electrical conductivity σ_e in a rectangular enclosure of height H as shown in Fig. 1. The right and the left walls are maintained at uniform temperatures T_H and T_C, respectively, and are such that $T_H > T_C$. The upper and lower boundaries are considered to be adiabatic or insulated. We also bring into account the effect of a uniform volumetric heat generation, q''' [W·m^{-3}], in the flow region.

We further assume that the cavity is permeated by a uniform magnetic field $\mathbf{B} = B_x \mathbf{e}_x + B_y \mathbf{e}_y$ (where B_x and B_y are space independent) of constant magnitude $B_0 = \sqrt{(B_x^2 + B_y^2)}$ and $\mathbf{e}_x$ and $\mathbf{e}_y$ are unit vectors in Cartesian coordinate system. The orientation of the magnetic field forms an angle ϕ with horizontal axis, such that $\tan\phi = B_y/B_x$. The electric current $\mathbf{J}$ and the electromagnetic force $\mathbf{F}$ are defined by

$$\mathbf{J} = \sigma_e(-\nabla\varphi + \mathbf{V} \times \mathbf{B}) \tag{1a}$$

$$\nabla \cdot \mathbf{J} = 0 \tag{1b}$$

$$\mathbf{F} = \mathbf{J} \times \mathbf{B} \tag{1c}$$

where φ is the electric potential and $\mathbf{V} = u\mathbf{e}_x + v\mathbf{e}_y$ is the field velocity. Here Eq. (1a) is Ohm's law and (1b) is the conservation of electric current. With electrically insulated boundaries in the present two-dimensional flow the electric potential φ is constant (please see [15]) and hence we have

$$\mathbf{J} = \sigma_e(\mathbf{V} \times \mathbf{B}) \tag{2a}$$

Which then reduce (1c) to

$$\mathbf{F} = \sigma_e(\mathbf{V} \times \mathbf{B}) \times \mathbf{B} \tag{2b}$$

We also assume that the surface tension, σ, varies linearly with temperature as given below:

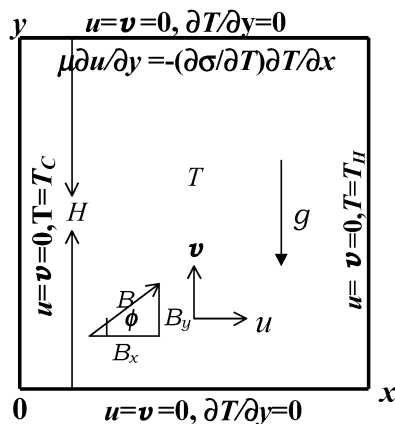$$\sigma = \sigma_0\big[1 - \gamma(T - T_0)\big] \tag{3}$$

Fig. 1. The flow configuration and coordinate system.

where $T_0 = (T_H + T_C)/2$ is the mean of the temperatures of heated and cold surface,

$$\gamma = (1/\sigma_0)(\partial\sigma/\partial T)$$

is the temperature coefficient of the surface tension, σ_0 is a reference surface tension and T is the temperature of the fluid in the cavity. Further it is assumed that, the upper boundary is flat and the fluid above the surface is assumed to be a gas of negligible viscosity and conductivity, and therefore it will not influence the flow and temperature fields in the fluid. Finally, the direction of the gravitational force is as indicated in Fig. 1.

Under the above assumptions, the conservation equations for mass, momentum and energy in a two-dimensional Cartesian co-ordinate system are [15]:

$$\frac{\partial u}{\partial x} + \frac{\partial v}{\partial y} = 0 \tag{4}$$

$$\frac{\partial u}{\partial t} + u\frac{\partial u}{\partial x} + v\frac{\partial u}{\partial y}$$
$$= -\frac{1}{\rho}\frac{\partial p}{\partial x} + \nu\nabla^2 u + \frac{\sigma_e B_0^2}{\rho}(v\sin\phi\cos\phi - u\sin^2\phi) \tag{5}$$

$$\frac{\partial v}{\partial t} + u\frac{\partial v}{\partial x} + v\frac{\partial v}{\partial y}$$
$$= -\frac{1}{\rho}\frac{\partial p}{\partial y} + \nu\nabla^2 v + \frac{\sigma_e B_0^2}{\rho}(u\sin\phi\cos\phi - v\cos^2\phi)$$
$$+ g\beta(T - T_0) \tag{6}$$

$$\frac{\partial T}{\partial t} + u\frac{\partial T}{\partial x} + v\frac{\partial T}{\partial y} = \alpha\nabla^2 T + \frac{q'''}{\rho C_p} \tag{7}$$

where ∇^2 is the Laplacian, u and v are the fluid velocity components in the x- and y-direction, respectively, T is the time, p is the fluid pressure, β is the volumetric thermal expansion coefficient, ρ, α and C_p are, respectively, the density of the fluid, the thermal diffusivity, and the specific heat at constant pressure.

In the present problem the effect of the induced electric current on the imposed field and the Joulean heating are neglected. This is justified as an estimation of the non-dimensional parameter characteristic for liquid metals and semiconductors, which is the ratio of the induced and imposed magnetic fields and known as the magnetic Prandtl number, Pm, for liquid metals and semi-conductor melts is O(10^{-7}) [15].

The boundary conditions for the present problem can now be given as

$$u = v = T = 0 \quad \text{for } t = 0$$
$$u = v = 0, \qquad T = T_H \quad \text{for } 0 \leqslant y \leqslant H \text{ at } x = L$$
$$u = v = 0, \qquad T = T_C \quad \text{for } 0 \leqslant y \leqslant H \text{ at } x = 0 \tag{8}$$
$$u = v = 0, \qquad \frac{\partial T}{\partial y} = 0 \quad \text{for } 0 \leqslant x \leqslant H \text{ at } y = 0$$

The conditions at the upper free surface are

$$u = v = 0, \qquad \frac{\partial T}{\partial y} = 0, \qquad \mu \frac{\partial u}{\partial y} = -\frac{\partial \sigma}{\partial T} \frac{\partial T}{\partial x}$$

$$\text{for } 0 \leqslant x \leqslant H \text{ at } y = H \tag{9}$$

The dynamic boundary conditions on the upper free surface (i.e., at $y = H$) relates the velocity gradient to the temperature gradient and this represents the balance between the shear-stress and the surface tension gradient at the surface which is responsible for establishment of thermo-capillary flow in the cavity.

It should be noted that the effect of interface deformability on the onset of instability has not been investigated. Its influence on the flow velocity has been given by Strani et al. [22] for the steady state regime. The shape of the gas–liquid interface in a square cavity has been computed by Cuvelier and Driessen [26] for different values of driving forces, such as the buoyancy force and the pressure force. For pure buoyancy flow, the pressure is higher in the upper hot corner and consequently there is an elevation of the free boundary in this corner and a depression near the cold corner. For pure thermocapillary flow the opposite effect has been observed. For combined convection the free surface was found to be flattened by increasing the Bond number, $B_0 (= \rho g H^2 / \sigma_0)$. Cuvelier and Driessen [23] also showed that the free-surface shape depends strongly on the Ohnesorage number $(Oh = \mu / (\rho \sigma_0 H)^{1/2})$.

Now, we construct the following dimension less variables:

$$X = \frac{x}{H}, \qquad Y = \frac{y}{H}, \qquad \tau = \frac{t}{H^2 / v}$$

$$U = \frac{u}{v/H}, \qquad V = \frac{v}{v/H}, \qquad \theta = \frac{T - T_0}{T_H - T_0} \tag{10}$$

Introducing the above dimensionless dependent and independent variables into the governing equations (4)–(8) yields the following equations:

$$\frac{\partial \Omega}{\partial \tau} + \frac{\partial (U \Omega)}{\partial X} + \frac{\partial (V \Omega)}{\partial Y}$$
$$= \nabla^2 \Omega + \frac{1}{2} Gr \frac{\partial \theta}{\partial X} + Ha^2 \left[\sin \phi \cos \phi \left(\frac{\partial U}{\partial X} - \frac{\partial V}{\partial Y} \right) \right.$$
$$\left. + \left(\sin^2 \phi \frac{\partial U}{\partial Y} - \cos^2 \phi \frac{\partial V}{\partial X} \right) \right] \tag{11}$$

$$\frac{\partial \theta}{\partial \tau} + \frac{\partial (U \theta)}{\partial X} + \frac{\partial (V \theta)}{\partial Y} = \frac{1}{Pr} \nabla^2 \theta + \frac{\lambda}{Pr} \tag{12}$$

where

$$\Omega = -\nabla^2 \psi \tag{13}$$

is the vorticity function and ψ is the stream function defined by:

$$U = \frac{\partial \psi}{\partial Y}, \qquad V = -\frac{\partial \psi}{\partial X} \tag{14}$$

The dimensionless initial and boundary conditions are:

$$U = V = \psi = \theta = 0 \quad \text{for } \tau = 0$$

$$U = V = \psi = 0, \qquad \theta = -1 \quad \text{for } 0 \leqslant Y \leqslant 1 \text{ at } X = 0$$

$$U = V = \psi = 0, \qquad \theta = +1 \quad \text{for } 0 \leqslant Y \leqslant 1 \text{ at } X = A$$

$$U = V = \psi = 0, \qquad \frac{\partial \theta}{\partial Y} = 0 \quad \text{for } 0 \leqslant X \leqslant 1 \text{ at } Y = 0$$

$$U = V = 0, \qquad \frac{\partial \theta}{\partial Y} = 0, \qquad \Omega = \frac{\partial U}{\partial Y} = -\frac{Ma}{2Pr} \frac{\partial \theta}{\partial X}$$

$$\text{for } 0 \leqslant X \leqslant 1 \text{ at } Y = 1 \tag{15}$$

In the above equations $A = L/H$ and Gr, Pr, λ, Ha and Ma are, respectively, the Grashof number, Prandtl number, heat generation parameter, Hartmann number and the Marangoni number which are defined as given below:

$$Gr = \frac{g \beta_T (T_H - T_C) H^3}{v^2}, \qquad Pr = \frac{v}{\alpha}, \qquad \lambda = 2 \frac{Ra_I}{Ra}$$

$$Ha^2 = \frac{B_0^2 H^2 \sigma_e}{\mu}, \qquad Ma = -\frac{\partial \sigma}{\partial T} \frac{T_H - T_C}{\mu \alpha} \tag{16}$$

In (16) $Ra_I = g \beta q''' H^5 / k \alpha v$ is the internal Rayleigh number since it depends on the volumetric heat generation q'''.

Once we know the numerical values of the temperature θ we may obtain the rate of heat flux from each of the walls since the non-dimensional heat flux from any surface is given by $-(\partial T / \partial n)$, where n is the direction normal to the wall. For example, the non-dimensional heat transfer rate in terms of local Nusselt number, Nu, from the right vertical heated surface is given by

$$Nu = \frac{1}{2} \frac{q H}{k (T_H - T_C)} = -\frac{1}{2} \left(\frac{\partial \theta}{\partial X} \right)_{X=A} \tag{17}$$

The corresponding value of the average Nusselt number, denoted by Nu_{av}, may be calculated from the following relation:

$$Nu_{av} = -\frac{1}{2} \int_0^1 \left(\frac{\partial \theta}{\partial X} \right) dY \tag{18}$$

3. Numerical solution methodology

An upwind finite-difference method, together with a successive over-relaxation iteration (SOR) technique, has been employed to integrate the model equations (11) and (14) subject to the boundary conditions given in (15). To do this, the first and second derivatives were approximated by central differences and were used in the vorticity, energy and Poisson equations. To preserve the conservative property, the finite difference forms of the vorticity and energy equations were written in conservative form for the convective terms as defined by Roache [24]. For the solution of the vorticity equation the values of the vorticity at the wall were needed. The wall vorticity were obtained by expanding the stream function in a Taylor series. We then obtained the wall vorticities as follows (for further details see Roache [24]):

$$\Omega_w = -2 \psi_{w+1} / \Delta w$$

where w and $w+1$ are respectively the grid points at the wall and close to the wall, and Δw is the space between these two grid points. Values of the streamfunction at all grid points were obtained with Eq. (13) via a successive over-relaxation method. All values for the relaxation parameters were between 1.82 and 1.89. The velocities at all grid points were determined with the dimensionless form of Eq. (14) using updated values of the stream function. Variations by less than 10^{-4} over all grid points for the streamfunction were adopted as the convergence criterion.

It is clear that the non-dimensional parameters of interest are the Grashof number, Gr, the Prandtl number, Pr, the heat generation parameter, λ, the Marangoni number, Ma, the Hartmann number, Ha, and ϕ the direction of the external magnetic field. In the present investigation, pertaining to liquid metal, the value of the Prandtl number is chosen to be 0.054 and the Grashof number is taken to be 2×10^5. The aspect ratio considered is unity and the value of the grid length is denoted by $h\ (=1/n$, where n is the number of grid points in both the X and Y directions for square cavity).

The results, which are shown and discussed in the following sections, have been calculated from zero initial velocities and mean values of temperature. A grid dependence study has been carried out, as in Hossain and Wilson [25] and Hossain and Rees [26] for a thermally-driven cavity flow, for different values of the physical parameters, with meshes of 41×41, 51×51 and 61×61 points. It has been found that there are very small differences in the maximum or minimum values of the stream-function between above sets of meshes. Hence we have chosen to use 51×51 mesh points throughout the present computations for $\tau = 0.1$ with a time step of 5×10^{-6}, which was found to be sufficient to reach the steady-state situation for the fluid of $Pr = 0.054$. In Fig. 2 we demonstrate the values of the average Nusselt number, Nu_{av}, along the heated surface of a square cavity, against τ. In this figure the graphs are for Gr equal to 2×10^4, 2×10^5 and 2×10^6 while values of all other physical parameters are zero. It is seen that the numerical values of Nu_{av} reach their respective steady values long before $\tau = 0.1$. However, throughout the present computations we have taken the value of $\tau = 0.1$.
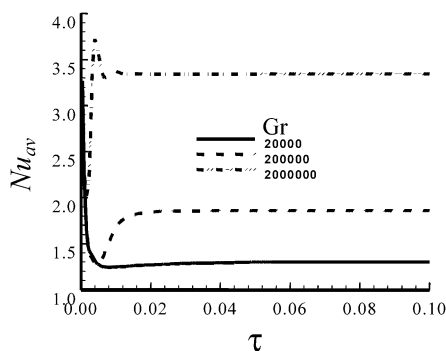
4. Results and discussion

Numerical results are presented in order to determine the effects of the presence of a magnetic field, volumetric heat generation and different Marangoni numbers on the natural convection flow of an electrically conducting fluid in a square cavity. Values of the magnetic field parameter Ha range between 0.0 to 40.0, the internal heat-generation parameter, λ, between 0.0 and 60.0 but for the Marangoni number, Ma, equal to 1000 and. Typical value of direction of the external magnetic field with the horizontal considered to be $\phi\ (=0, \pi/4, \pi/2, 3\pi/4)$.

4.1. Comparison with earlier investigations

The corresponding problem of natural convection flow, without heat generation, but in presence of a uniform magnetic field acting in the direction of the cavity (i.e., for the case $\phi = \pi/2$) both with and without the effect of thermocapillary force has already been investigated by Rudraiah et al. [27]. In that investigation a finite difference method together with ADI was employed for different values of the Grashof number, Gr, Hartmann number, Ha, and Marangoni number, Ma, for a fluid with Prandtl number, $Pr = 0.733$. Typical results obtained by the above authors has been revisited by the present authors for the following values of the physical parameters: $Gr = 2 \times 10^6$, $Pr = 0.733$, $Ha = 20$ and $\phi = \pi/2$; these were found to be in excellent agreement. We also revisited the case for which $Gr = 2 \times 10^4$, $Pr = 0.054$ and $Ma = 100$ with $Ha = 0$ and $\lambda = 0$ in the model considered in Ref. [16] using the present method. In this case also we found an excellent agreement with the results of [16] qualitatively as shown in Fig. 3.

Finally, the authors considered an aspect ratio 4 cavity subject to a heated left-wall $(\theta = 1)$ and a cold right wall $(\theta = 0)$ with the parameter values: $\varphi = 0$, $Gr = 5.37 \times 10^6$, $Pr = 0.015$, $Ha = 20$, $Ma = 0$ and $\lambda = 0$; this particular case has been investigated by Gelfgat and Yoseph [15]. In this case also we found an extremely close match with the results obtained by Gelfgat and Yoseph [15], which are reproduced in Fig. 4.

So we believe that the present method yields sufficiently accurate results and is computationally efficient.

Fig. 2. Average Nu_{av}, at the right heated surface against τ for different Gr while $Ma = 1000$, $Ha = 0$, $\alpha = 0$ and $\lambda = 0$.
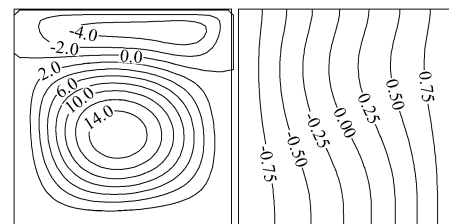

Fig. 3. Streamlines and isotherms for $Gr = 2 \times 10^4$ and $Pr = 0.054$ and $Ma = 100$ while $Ha = 0$ and $\lambda = 0$ [16].
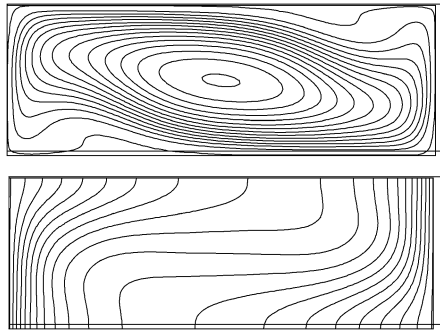
Fig. 4. Streamlines (top) and isotherms (bottom) with left heated-wall and right cold-wall while $Gr = 5.37 \times 10^6$, $Pr = 0.015$, $Ha = 20$, $Ma = 0$, $\varphi = 0.0$ (Gelfgat and Bar-Yoseph [15]).

## 4.2. Effects of varying the Grashof and Hartmann numbers on the flow field and the heat transfer

We consider first the effect of an external magnetic field acting in the direction parallel to the horizontal (i.e., $\phi = 0$) with surface tension effects at the top surface (while $Ma = 1000$) but without internal heat generation ($\lambda = 0$). The resulting flow and temperature distributions are depicted in Fig. 5. In Fig. 5(a) we depict the streamlines for increasing values of the Grashof number: 2×10^4, 2×10^5 and 2×10^6 while the Hartmann number, Ha, and the Marangoni number, Ma, were taken as 20 and 1000, respectively. In this figure we see the presence of two cells. The upper cell has developed along the top surface of the domain because of the presence of thermocapillary forces. From the streamlines one may also see that the size of the upper cell and the flow rate there gradually decreases with the increase of the value of the buoyancy parameter, Gr. This is possible, since an increase in the value of Gr will increase the dominancy of the buoyancy force over the present magnetic field strength and the thermo-capillary force.

The corresponding effect of the increasing buoyancy forces on the isotherms are shown in Fig. 5(b). From this figure we can ascertain that increase in the buoyancy force causes the isotherms to deform increasingly, and thin thermal boundary layers form near both the heated and cooled surfaces. This is because increasing buoyancy forces increase the fluid velocity up the heated surface, and therefore heat cannot conduct so far perpendicular to the surface. Thus thin layers form which are associated with high rates of heat transfer. This effect of the increasing buoyancy force on the local heat transfer from the heat surface is depicted in Fig. 10(a).

Fig. 6(a) depicts the streamlines with effect of increasing values of magnetic field parameter while the magnetic field applied in the direction parallel to the horizontal (i.e., $\phi = 0$). From the figures, it can be seen that intensities in both the primary and secondary flow decrease owing to increase in the magnetic field. This is expected since presence of magnetic field usually retards the velocity field. The corresponding effect of the increasing magnetic field on the
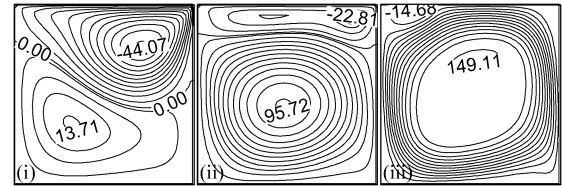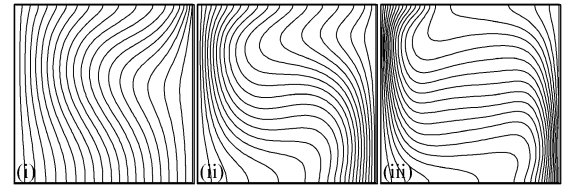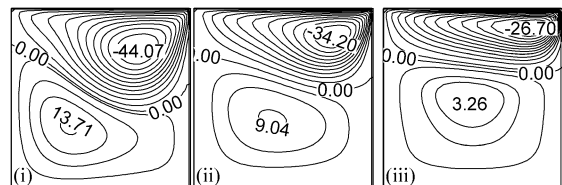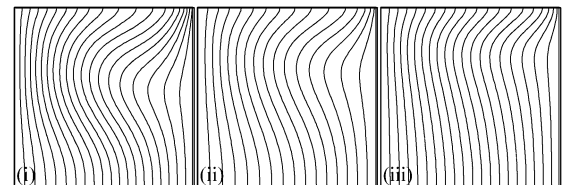

Fig. 5. Steady state (a) streamlines and (b) isotherms for (i) $Gr = 2 \times 10^4$ (ii) $Gr = 2 \times 10^5$ and (iii) $Gr = 2 \times 10^6$ while $Ma = 1000$, $Ha = 20$, $\phi = 0$ and $\lambda = 0$.

Fig. 6. Steady state (a) streamlines and (b) isotherms for (i) $Ha = 0$, (ii) $Ha = 20$ and (iii) $Ha = 40$ while $Gr = 2 \times 10^4$, $Ma = 1000$, $\phi = 0$ and $\lambda = 0$.

isotherms may be viewed in Fig. 6(b). It may be seen that the isotherms become more vertical and straighten out due to the increase of the magnetic field strength, which is expected; since the magnetic field resists the flow, as observed above. This effect can also be seen in Fig. 10(b).

4.3. Effect of the direction of the external magnetic field on the flow and the temperature distribution

Now we discuss the effect of the direction of the external magnetic field on the flow and the temperature distribution. Our results are shown in the form of streamlines and isotherms in Figs. 7 and 8, respectively. Fig. 7 represents the streamlines at the steady state situation, which was attained at times of less then 0.1, for $\phi = 0$, $\pi/4$ and $\pi/2$ while $Gr = 2 \times 10^4$, $Ma = 1000$ and $Ha = 20$. It can be see from this that, as the direction of the external magnetic changes from horizontal to vertical, the flow rate in both the primary and the secondary cells decreases which causes an increase in the effect of the thermocapillary force. But at higher val-

ues of the buoyancy force (the case when $Gr = 2 \times 10^5$) the effect of the direction of the magnetic field is so significant as the flow is dominated much more by the strength of the buoyancy force.

The corresponding isotherms are depicted in Fig. 8. In this figure, for both values of the buoyancy parameter, Gr, one can see that as the direction of the external magnetic
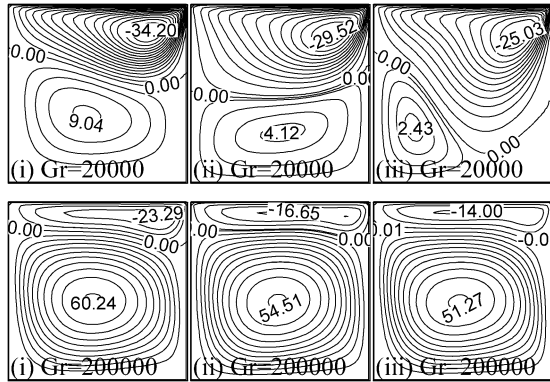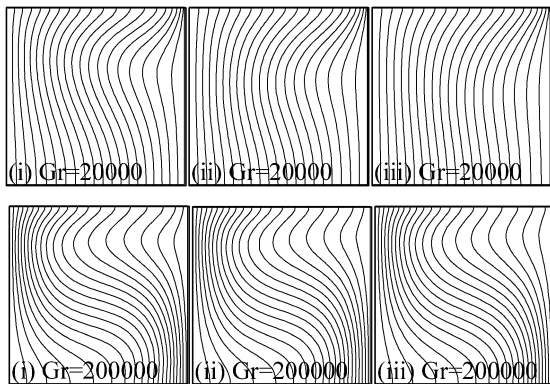
field changes from 0 to $\pi/4$, the isotherms near the heated surface become parabolic; whereas a further change of the direction to $\pi/2$, that is when the magnetic field acts in the vertical direction, the isotherms near the heated surface become similar to the case of the horizontal magnetic field. All these because change in the direction reduces the flow rate in the cells which results the reduction of heat transfer rate from the heated surface.

4.4. Effects of internal heat generation on the flow field and the heat transfer

Now we discuss the effects of the internal heat generation parameter (λ) on the flow and heat transfer on the natural convection flow on taking $Gr = 2 \times 10^4$, $Ma = 1000$ and $Ha = 20$.

Fig. 9(a) depicts the streamlines for values of heat generation parameter $\lambda = 0.0$, 10, 20, 40 and 60. From these figures we may see that increasing values of the heat generation parameter leads increasing flow rates in the primary cell as well an increase in its size until it occupies almost all of the total cavity space. The increasing rate of heat generation also causes the development of another secondary cell at the top-right corner of the cavity. The flow strength in this new cell also increases when the internal heat generation increases in magnitude. On the other hand, the secondary cell that exists near the lower surface of the cavity gradually disappears when the heat generation parameter, λ, increases. This effect of internal heat generation on the flow field is reasonable since internal heat generation assists buoyancy forces by accelerating the fluid flow. This effect we see in Fig. 9(b). On the other hand, the increase in the temperature of the fluid due to the increasing rate of internal heat generation negates the heat transfer from the heated surface. In Fig. 12, we see the corresponding effects of the increase of the internal heat generation on the surface heat transfer from the heated surface of the cavity.
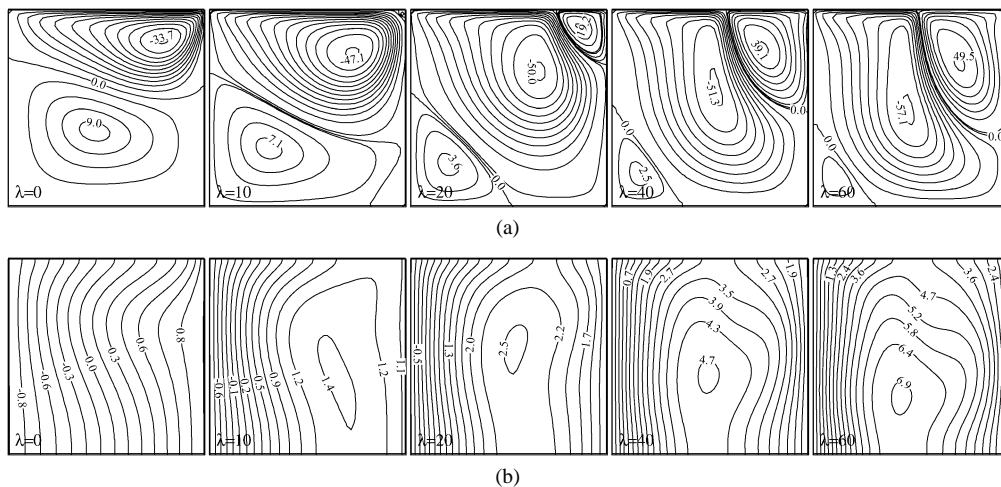

Fig. 7. Steady state streamlines for (i) $\phi = 0$, (ii) $\phi = \pi/4$ and (iii) $\phi = \pi/2$ while $Gr = 2 \times 10^4$ and 2×10^5, $\lambda = 0$, $Ma = 1000$ and $Ha = 20$.

Fig. 8. Steady state isotherms for (i) $\phi = 0$, (ii) $\phi = \pi/4$ and (iii) $\phi = \pi/2$ while $Gr = 2 \times 10^4$ and 2×10^5, $\lambda = 0$, $Ma = 1000$ and $Ha = 20$.

(a)

(b)

Fig. 9. Steady state (a) streamlines and (b) isotherms for different λ while $Gr = 2 \times 10^4$, $Ha = 20$, $Ma = 1000$ and $\phi = 0$.
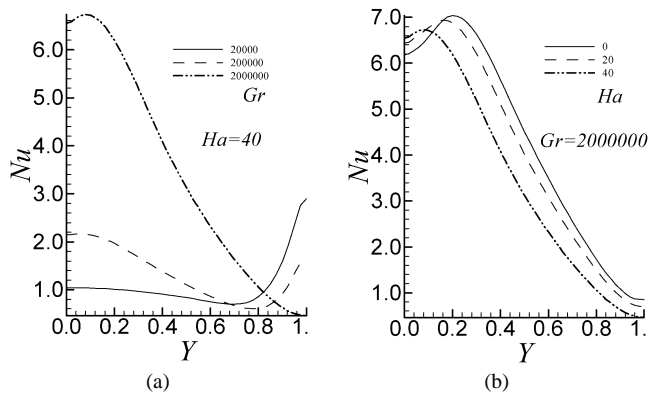
Fig. 10. Numerical values of local Nusselt number, *Nu*, at the right heated surface for different *Gr* while *Ha* = 0.0 and different *Ha* while *Gr* = 2 × 10⁵, *Ma* = 1000, λ = 0, φ = 0.
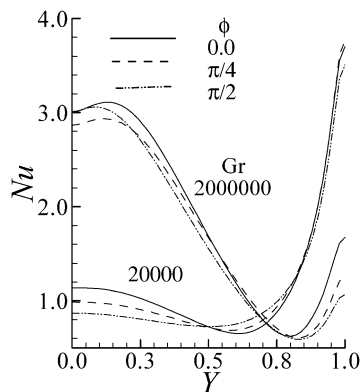

Fig. 11. Numerical values of local Nusselt number, *Nu*, at the right heated surface for different φ while *Gr* = 2 × 10⁴ and 2 × 10⁵, *Ma* = 1000, *Ha* = 20 and λ = 0.
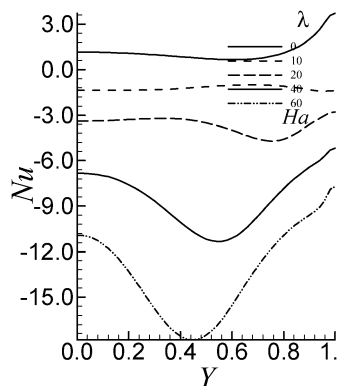

Fig. 12. Numerical values of local Nusselt number, *Nu*, at the right heated surface for different λ while *Ma* = 1000 and *Gr* = 2 × 10⁴, *Ha* = 20 and φ = 0.

5. Concluding remarks

In the present paper a problem on combined buoyancy and thermo-capillary convection flow of electrically conducting fluid filled in an enclosure under an externally imposed uniform magnetic field including the additional effect of internal heat generation has been investigated numerically by employing an upwind finite difference method together with a successive over-relaxation (SOR) technique. Choosing a fluid of small Prandtl number ($Pr = 0.054$, which is appropriate for liquid metal and semi-conductor melts) and a Marangoni number, $Ma(= 1000)$, solutions have been obtained for values of the Grashof number, *Gr*, equal to 2×10^4, 2×10^5 and 2×10^6 and that of Hartmann number, *Ha*, which ranges from 0.0 to 40 and the heat generation parameter, λ, ranges from 0.0 to 40.

The following conclusions may be drawn from the present investigations:

- change of direction of the external magnetic force from horizontal to vertical leads to decrease in the flow rates in both the primary and the secondary cells and that causes an increase in the effect of the thermocapillary force.
- increase in the value of the heat generation parameter leads to increase in the flow rates in the primary cell as well an increase in its size until it occupies almost all of the total cavity space. Further increase in the value of heat generation causes for development of more cells in the cavity.
- the temperature of the fluid in the cavity also increases due to the increase of internal heat generation and hence that negates the heat transfer from the heated surface.

Finally, it requires to be mentioned that solutions of the present problem could be investigated for a fluid having any further smaller values of *Pr*.

References

[1] S. Ostrach, Fluid mechanics in crystal growth—the 1982 Freeman Scholer lecture, J. Fluids Engrg. 105 (1983) 5–20.
[2] S.M. Pimputkar, S. Ostrach, Convective effects in crystal grown from melt, J. Crust. Growth 55 (1981) 614–646.
[3] S. Ostrach, Low-gravity fluid flows, Annual Rev. Fluid Mech. 14 (1988) 313–345.
[4] T.L. Bergman, S. Ramadhyani, Combined buoyancy and thermocapillary driven convection in open square cavities, Numer. Heat Transfer 9 (1986) 441–451.
[5] J. Srinivasan, B. Basu, A numerical study of thermocapillary flow in a rectangular cavity during laser melting, Internat. J. Heat Mass Transfer 29 (1986) 563–572.
[6] B. Basu, J. Srinivasan, Numerical study of steady-state laser melting problem, Internat. J. Heat Mass Transfer 31 (1988) 23–31.
[7] J.C. Chen, Y.C. Huang, Thermocapillary flows of surface melting due to a moving heat flux, Internat. J. Heat Mass Transfer 34 (1990) 663–671.

[8] B.M. Carpenter, G.M. Homsy, Combined buoyant thermocapillary flow in a cavity, J. Fluid Mech. 207 (1989) 121–132.

[9] H. Ben Hadid, B. Roux, Buoyancy and thermocapillary driven flows in differentially heated cavities for low-Prandtl number fluids, J. Fluid Mech. 235 (1992) 1.

[10] A. Juel, T. Mullin, H. Ben Hadid, D. Henry, Magnetohydrodynamic convection in molten gellium, J. Fluid Mech. 378 (1999) 97–118.

[11] H. Ben Hadid, D. Henry, H. Kaddeche, Numerical study of convection in the horizontal Bridgman configuration under the action of a constant magnetic field, Part 1: Two dimensional flow, J. Fluid Mech. 333 (1997) 23–56.

[12] H. Ben Hadid, D. Henry, Numerical study of convection in the horizontal Bridgman configuration under the action of a constant magnetic field, Part 2: Three dimensional flow, J. Fluid Mech. 333 (1997) 57–83.

[13] R. Moessner, U. Mueller, A numerical Investigation of three-dimensional magneto-convection in rectangular cavities, Internat. J. Heat Mass Transfer 42 (1999) 1111–1121.

[14] J. Priede, G. Gerbeth, Hydro-thermal wave instability of thermocapillary driven convection in a coplanar magnetic field, J. Fluid Mech. 347 (1997) 141–169.

[15] A.Y. Gelfgat, P.Z. Bar-Yoseph, Effect of an external magnetic field on oscillatory instability of convective flows in rectangular cavity, Phys. Fluid 13 (2001) 2269–2278.

[16] N. Rudraiah, M. Venkatachalappa, C.K. Subbaraya, Combined surface tension and buoyancy-driven convection in a rectangular open cavity in the presence of a magnetic field, Internat. J. Non-Linear Mech. 30 (5) (1995) 759.

[17] S. Kakac, W. Aung, R. Viskanta, Natural Convection—Fundamentals and Applications, Hemisphere, Washington, DC, 1985.

[18] S. Acharya, R.J. Goldstein, Natural convection in an externally heated vertical or inclined square box containing internal energy sources, ASME J. Heat Transfer 107 (1985) 855–866.

[19] A.G. Churbanov, P.N. Vabishchevich, V.V. Chudanov, V.F. Strizhov, A numerical study on natural convection of a heat generating fluid in rectangular enclosures, Internat. J. Heat Mass Transfer 37 (1994) 2969–2984.

[20] K. Vajravelu, J. Nayfeh, Hydromagnetic convection at a cone and a wedge, Internat. Comm. Heat Mass Transfer 19 (1992) 701–710.

[21] A.J. Chamkha, H. Al-Naser, Hydromagnetic double-diffusive convection in a rectangular enclosure with uniform side heat and mass fluxes and opposing temperature and concentration gradients, Internat. J. Thermal Sci. 41 (2002) 936–948.

[22] M. Strani, R. Piva, G. Graziani, Thermocapillary convection in a rectangular cavity: asymptotic theory and numerical simulation, J. Fluid Mech. 130 (1983) 347–376.

[23] C. Cuvelier, J.M. Driessen, Thermocapillary free boundaries in crystal growth, J. Fluid Mech. 169 (1986) 1–26.

[24] P.J. Roache, Computational Fluid Dynamics, Hermosa, Albuquerque, NM, 1972.

[25] M.A. Hossain, M. Wilson, Natural convection flow in a fluid saturated porous medium enclosed by non-isothermal walls with heat generation, Internat. J. Thermal Sci. 41 (2002) 447–454.

[26] M.A. Hossain, D.A.S. Rees, Natural convection flow of a viscous incompressible fluid in a rectangular porous cavity heated from below with cold sidewalls, Heat Mass Transfer 39 (2003) 657–663.

[27] N. Rudraiah, R.M. Barron, M. Venkatachalappa, C.K. Subbaraya, Effect of magnetic field in a rectangular enclosure, Internat. J. Engrg. Sci. 33 (1995) 1075–1084.